Available online at www.sciencedirect.com

ScienceDirect

www.elsevier.com/locate/jes

JES JOURNAL OF ENVIRONMENTAL SCIENCES

www.jesc.ac.cn

Remediation of preservative ethylparaben in water using natural sphalerite: Kinetics and mechanisms

Yanpeng Gao[1,2,3], *Teng Guo*[1,2], *Xiaolin Niu*[1,2], *Na Luo*[1,2], *Jia Chen*[1,2], *Junlang Qiu*[3], *Yuemeng Ji*[1,2], *Guiying Li*[1,2], *Taicheng An*[1,2,*]

[1] *Guangdong-Hong Kong-Macao Joint Laboratory for Contaminants Exposure and Health, Guangdong Key Laboratory of Environmental Catalysis and Health Risk Control, Institute of Environmental Health and Pollution control, Guangdong University of Technology, Guangzhou 510006, China*

[2] *Guangzhou Key Laboratory of Environmental Catalysis and Pollution Control, Key Laboratory of City Cluster Environmental Safety and Green development, School of Environmental Science and Engineering, Guangdong University of Technology, Guangzhou 510006, China*

[3] *Division of Analytical and Environmental Toxicology, Department of Laboratory Medicine and Pathology, Faculty of Medicine and Dentistry, University of Alberta, Edmonton, AB T6G 2G3, Canada*

ARTICLE INFO

Article history:
Received 3 April 2021
Revised 19 May 2021
Accepted 19 May 2021

Keywords:
Emerging organic contaminants
Paraben
Naturally abundant minerals
Natural sphalerite
Adsorption mechanism

ABSTRACT

As a typical class of emerging organic contaminants (EOCs), the environmental transformation and abatement of preservative parabens have raised certain environmental concerns. However, the remediation of parabens-contaminated water using natural matrixes (such as, naturally abundant minerals) is not reported extensively in literature. In this study, the transformation kinetics and the mechanism of ethylparaben using natural sphalerite (NS) were investigated. The results show that around 63% of ethylparaben could be absorbed onto NS within 38 hr, whereas the maximum adsorption capacity was 0.45 mg/g under room temperature. High temperature could improve the adsorption performance of ethylparaben using NS. In particular, for the temperature of 313 K, the adsorption turned spontaneous. The well-fitted adsorption kinetics indicated that both the surface adsorption and intra-particle diffusion contribute to the overall adsorption process. The monolayer adsorption on the surface of NS was primarily responsible for the elimination of ethylparaben. The adsorption mechanism showed that hydrophobic partitioning into organic matter could largely govern the adsorption process, rather than the ZnS that was the main component of NS. Furthermore, the ethylparaben adsorbed on the surface of NS was stable, as only less than 2% was desorbed and photochemically degraded under irradiation of simulated sunlight for 5 days. This study revealed that NS might serve as a potential natural remediation agent for some hydrophobic EOCs including parabens, and emphasized the significant role of naturally abundant minerals on the remediation of EOCs-contaminated water bodies.

Introduction

The occurrence of emerging organic contaminants (EOCs) in water and sediments has already become a global concern

* Corresponding author.
E-mail: antc99@gdut.edu.cn (T. An).

https://doi.org/10.1016/j.jes.2021.05.030
1001-0742/

(Gao et al., 2016; Mitch, 2017; Schwarzenbach et al., 2010). As an important group of EOCs, parabens are often used as additives to induce antimicrobial characteristics in certain streams of pharmaceuticals, cosmetics, and food-stuffs (Brausch and Rand, 2011; Chen et al., 2017; Liao et al., 2013). The annual consumption of parabens was estimated to be about 8000 tons around the world (Ramaswamy et al., 2011). Furthermore, several parabens could inevitably enter water bodies due to incomplete elimination in wastewater treatment plants (WWTPs). As a result, parabens have been frequently detected in the effluents of WWTPs, surface water bodies, as well as sediments, and the corresponding concentrations have been reported to lie within the range of 15–400 ng/L (Cheng et al., 2018; González-Mariño et al., 2011; Kasprzyk-Hordern et al., 2008). Moreover, previous studies have found that parabens have potential adverse impacts on aquatic organisms and human health (An et al., 2014; Gao et al., 2016). For instance, parabens could impose endocrine-disrupting effects on human health, even at concentrations as low as ng/L (Haman et al., 2015), furthering the cancer-causing potential of parabens (Darbre and Harvey, 2008). More importantly, recent studies observed the increased aquatic toxicity and endocrine-disrupting characteristics during their ultraviolet (UV) photochemical degradation (Fang et al., 2013; Gao et al., 2020). Therefore, understanding the transformation mechanism and environmental fate of parabens in natural water bodies and sediments are very important for the risk assessment and protection of human health.

In recent years, several research groups have mainly focused on the degradation of parabens using UV irradiation, photocatalytic, electrochemical and ozone oxidation technologies (Dobrin et al., 2014; Fang et al., 2013; Frontistis et al., 2017; Gao et al., 2020; Petala et al., 2015). Parabens could be degraded relatively easily, however is often accompanied by incomplete mineralization and the consumption of extra energy (González-Mariño et al., 2011). The migration and transformation of various parabens in the natural aquatic environment is rarely studied, particularly with the remediation of parabens-contaminated water using natural matrices, such as natural minerals.

Natural minerals are an essential part of the environment. More importantly, several natural minerals exhibit excellent promise for participating in the transformation and/or purification of pollutants in the environmental field (Zhao et al., 2020), including the adsorption of lead using rock phosphate and that of proteins using montmorillonite (Prasad et al., 2000; Rytwo et al., 2010). Among natural minerals, certain special attention has been paid to natural sphalerite (NS) because of its adsorption capability and visible-light (VL) photocatalytic activity (Li et al., 2020). For instance, NS can inactivate bacteria and harmful algae upon visible light (VL) irradiation (Chen et al., 2011; Shen et al., 2020; Wang et al., 2017). Moreover, NS could perform as visible-light-driven (VLD) photocatalysts for reducing metal ions and degrading azo-dye and carbon tetrachloride (Li et al., 2009; Yan et al., 2006; Yang et al., 2011). In short, NS is a naturally occurring adsorbent and photocatalytic material that has the potential to be used to resolve traditional as well as metal-related environmental pollutions. However, for the increasingly serious EOCs, their transformation and environmental fate over the interface of NS minerals have not yet been studied.

In this study, ethylparaben was selected as a typical preservative of EOCs to evaluate their environmental behavior and final fate on NS minerals. Firstly, the adsorption processes were analyzed based on adsorption kinetics, adsorption isotherms, and adsorption thermodynamics. Total organic carbon (TOC), analysis of the surface area and pore size, fourier transform infrared (FT-IR) spectroscopy, and theoretical calculations were performed to explore the adsorption mechanism. Moreover, the potential secondary release and the stability of adsorbed NS were also measured as a result of the desorption of ethylparaben from the NS. Figuring out the kinetics and mechanism of the remediation of parabens-contaminated water using NS will help understand the environmental fate of parabens and further inspire more dramatic advancements in the field of natural remediation of pollutants.

1. Materials and methods

1.1. Materials

Ethylparaben (> 99.0%) was purchased from Tokyo Chemical Industry (Japan). NS was obtained from Huangshaping deposit in Hunan, China. NS used in the study was firstly crushed mechanically and milled at the mine. Then natural sphalerite powder (particle sizes $\leq$ 40 μm) was obtained by passing it through a 340-mesh sieve as used in earlier references (Chen et al., 2011; Li et al., 2020; Yang et al., 2011). As a contrast in the experiment, the nano-sized ZnS was obtained from Sigma-Aldrich. All solutions including ethylparaben stock solution were prepared using high-purity deionized water (18.2 MΩ cm; Millipore Corp., USA).

1.2. Adsorption and desorption experiments

Batch equilibrium tests were carried out for the adsorption of ethylparaben onto NS. The experiments for the adsorption kinetics were performed by adding 300 mg of NS into 100 mL Erlenmeyer flask, which contained 5 mg/L ethylparaben in a 50 mL solution. Samples were then shaken on an isothermal gas bath shaker with the rotational speed of 150 r/min at ambient temperature (25 $\pm$ 1 °C). These suspensions were harvested at preset time intervals. The suspensions were filtered using a syringe with a membrane (pore size: 0.22 μm) prior to analysis.

The concentrations of ethylparaben in the supernatant solutions before and after the adsorption were determined using a high-performance liquid chromatography (HPLC, Agilent 1260 series) with a photodiode array detector. The amount of ethylparaben adsorbed on NS at any time, q_t (mg/g), is given by Eq. (1).

$$q_t = \frac{(C_0 - C_t)v}{m} \quad (1)$$

where C_0 (mg/L) and C_t (mg/L) are the concentrations of ethylparaben in the solution at $t = 0$ and at any time t, respectively,

v (L) denotes the volume of ethylparaben solution, and m (g) represents the mass of NS added to the solution.

The experiments for adsorption isotherms were performed at adsorption equilibrium time. The initial concentration of ethylparaben solution lied within the range of 2–9 mg/L. The temperature effect on the adsorption process was studied by changing the process temperature through values of 298, 313, and 323 K. The solution temperature was adjusted using a controller on the gas bath shaker. The flasks in the shaker (at 150 rpm) were shaken at three different temperatures for 25 hr.

The adsorption experiments were performed in a 100 mL Erlenmeyer flask containing 50 mL of ethylparaben solution and 300 mg of adsorbent. The initial concentration of ethylparaben solution lied within the range of 2–9 mg/L. The flasks were consecutively shaken at 150 rpm in a shaker at the temperatures of 298, 313, and 323 K for 25 hr. Then, the suspensions were filtered using a syringe with the membrane (pore size: 0.22 μm) prior to analysis.

For desorption, the supernatant was removed and the same volumes of the background solution were used for correction (the operating time was kept to less than 3 min to minimize the potential loss due to volatilization during the replacement process). The flasks were sealed again and shaken. After achieving the equilibrium, the ethylparaben concentration was determined and the desorption efficiency of ethylparaben was evaluated.

1.3. *Photochemical degradation experiments*

Photochemical degradation kinetics of ethylparaben in NS slurry was conducted using a multi-channel system of photochemical reaction with visible light source ($\lambda \geq 420$ nm) (PCX50A Discover, Beijing Perfectlight Co., Ltd., China). The visible light irradiation was measured using a photometer (FZ-A, Perfect Light, China) and controlled to be 100 mW/cm^2. Considering the light intensity in the natural environment, the solar experiments were carried out under a 300-W Xenon lamp with a cut-off filter to simulate the visible light conditions. The visible light irradiation was measured to be 220 mW/cm^2. Photochemical degradation experiments were conducted using a 50 mL quartz bottle. In these experiments, 1 mL sample was periodically taken using a 0.22 μm syringe filter and used to analyze the concentration using HPLC.

1.4. *Measurement of the ethylparaben concentration*

The concentration of ethylparaben was monitored using a HPLC, equipped with a photodiode array detector. Separation was performed on an Agilent C18 column (4.6 × 250 mm, 5 μm particle diameter). The mobile phase (V_{water}:$V_{acetonitrile}$ = 50:50) was used to eluted at the flow rate of 0.5 mL/min and the temperature of 25 °C. A 10 μL aliquot of samples was injected, and the detection wavelength was set to be 254 nm.

1.5. *Data analysis and theoretical calculations*

In order to evaluate the kinetic sorption mechanism, the adsorption kinetics of ethylparaben on NS was fitted using the pseudo-first-order, pseudo-second-order, the Elovich, and the Weber-Morris kinetic models. Furthermore, the adsorption isotherm models were fitted using the Langmuir (Ghaffar et al., 2015), Freundlich (Freundlich, 1906), Dubinin-Radushkevich (Dubinin, 1947), and Redlich–Peterson isotherms (Redlich and Peterson, 1959). Finally, various thermodynamic parameters of the adsorption were calculated that included free energy (ΔG), enthalpy (ΔH), and entropy (ΔS) (Tan et al., 2009). All the equations of the models used in the current work are described in detail in Appendix A Text S1–S3. The electronic structure of ethylparaben was optimized using Gaussian 09 software (Frisch et al., 2009). The density functional method (DFT) was employed at B3LYP/6-31G(*d,p*), and the solvent effect was simulated using the recommended SMD model.

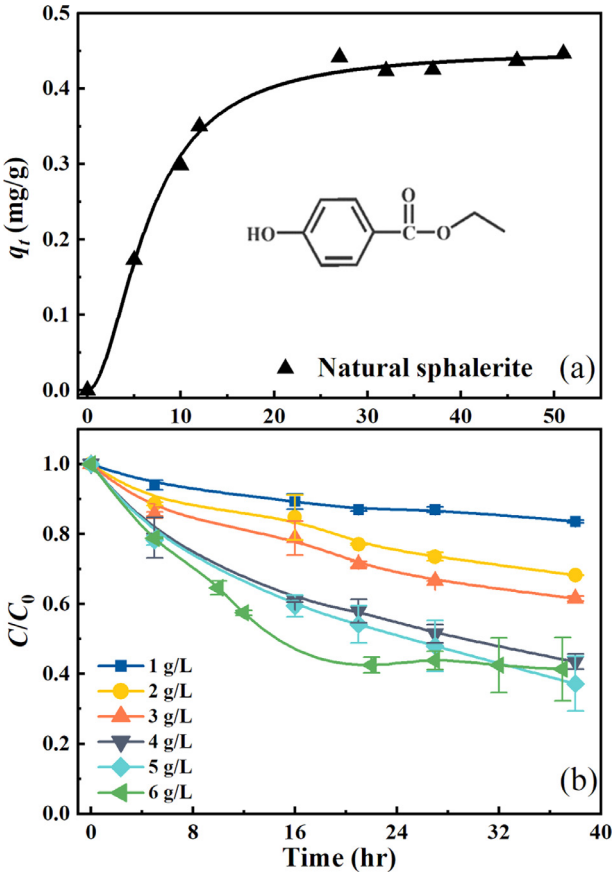

Fig. 1 – (a) The amount of ethylparaben adsorbed onto NS with the dose of 6 g/L and (b) Adsorption kinetics of ethylparaben on NS with the dose of 1–6 g/L.

2. Results and discussion

2.1. *Adsorption kinetics of ethylparaben onto NS*

Firstly, the adsorption kinetics of ethylparaben on NS with the concentration of 6 g/L was investigated. As shown in Fig. 1a, the apparent equilibrium was attained at approximately 50 hr. Approximately 78% of the ethylparaben was adsorbed within the initial 12 hr, and the adsorption amount was found to be

Table 1 – Comparison of pseudo-first-order; pseudo-second-order models and Elovich equation parameters, calculated $q_{e(cal)}$, and experimental $q_{e(exp)}$ values.

pseudo-first order			
k_1 (1/hr)	$q_{e(cal)}$ (mg/g)	$q_{e(exp)}$ (mg/g)	R^2
0.15	0.044	0.45	0.77
pseudo-second-order			
k_2 (g/mg hr)	$q_{e(cal)}$ (mg/g)	$q_{e(exp)}$ (mg/g)	R^2
0.28	0.51	0.45	0.97
Elovich equation			
$1/b$ (mg/g)	$q_{e(cal)}$ (mg/g)	$q_{e(exp)}$ (mg/g)	R^2
0.11	0.40	0.45	0.83

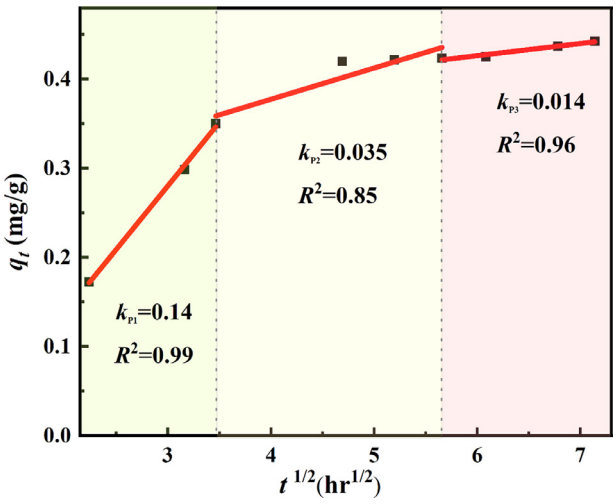

Fig. 2 – Plot of intraparticle diffusion Weber-Morris model for the adsorption of ethylparaben on NS.

0.35 mg/g. Then, the adsorption capacity increased slowly, and 97% adsorption was achieved within 38 hr. Finally, the equilibrium adsorption of 0.45 mg/g was achieved within 50 hr.

Furthermore, when the adsorbent dosage was increased from 1.0 to 5.0 g/L, the adsorption efficiency of ethylparaben increased from 17% to 63% within 38 hr (Fig. 1b). However, with further increase in the dosage of adsorbent to 6.0 g/L, the adsorption efficiency dropped to 59%. This is due to the reason that the agglomeration of NS at a high dosage of adsorbent could cause the coverage of adsorption sites, thereby reducing the capacity for the adsorption of ethylparaben. Therefore, it seems that the surface reactions and/or diffusion could be one of the significant factors to govern the adsorption of ethylparaben on NS.

In order to better examine the interaction of ethylparaben with NS, attempt was made to further elucidate the adsorption kinetics using three different kinetic models (Appendix A Figs. S1–S2). For instance, the pseudo-first-order model is often employed to describe the single layer of adsorption. The pseudo-second-order equation is considered as the chemisorption process (Eren and Acar, 2006; Tanis et al., 2008). The Elovich model describes the adsorption on heterogeneous surfaces, which is one of the most useful models for describing chemisorption (Aharoni and Tompkins, 1970). The three models are described in detail in Appendix A Text S1,S2, and their important parameters are listed in Table 1. Among the three models, the pseudo-second-order model exhibited the best fitting to the experimental data obtained in the current work. The obtained correlation coefficient (R^2 value) was 0.97, which was much higher than that of pseudo-first-order (0.77) and Elovich (0.83) models (Table 1). As a result, the adsorption process was considered to be dominated by chemisorption (Oleszczuk et al., 2009). In this case, the formation of covalent bonds between ethylparaben and NS minerals was expected. The functional groups on the surface of NS before and after the adsorption were determined using FT-IR spectroscopy, and the results are shown in Figs. S3a–c. A new peak around 3220 cm^{-1} was observed (Appendix A Fig. S3c), and represented the phenolic -OH stretch of parabens (Sustic, 1995). Additionally, the peaks in the vicinities of 1230 and 2350 cm^{-1} existed both before and after the adsorption (Appendix A Fig. S3a), indicating that they were the absorption peak of NS and/or organic matter. Based on a previous report (Bian et al., 2020). The peaks at 1230 cm^{-1} represented the C-N group of organic matter. Moreover, after the adsorption of ethylparaben (Appendix A Fig. S3b), the peaks slightly shifted to 2364 and 2342 cm^{-1}, respectively. The changes in these functional groups indicated that, when NS was exposed to ethylparaben, hydrocarbons could be the major adsorption sites (Kumar, 2015). Therefore, the hydrocarbons on the surface of natural sphalerite may interact with ethylparaben, and result in a weak red shift of the absorption peak.

In order to gain insight into the rate-controlling step for the ethylparaben adsorption on NS, the Weber-Morris model was used to examine the contribution of both surface and intraparticle diffusion to the kinetics (Ho, 2003). According to the model (Appendix A Text S2), intra-particle diffusion is the only rate-controlling step, provided the plot of up-take (q_e) against the square root of time ($t^{0.5}$) is linear and passes through the origin. However, the results showed that the fitted curve did not pass through the origin (Fig. 2), implying that the intraparticle diffusion was not the only factor governing the adsorption rate. Based on the fitted data (Fig. 2), it was found that the adsorption process consisted of three steps, which were as follows: (1) Due to the concentration-based driving force, the ethylparaben molecules transferred rapidly from the solution to the surface of NS. (2) The ethylparaben adsorbed on the surface of NS could pass through the pores, and then, diffused into the interior of NS. This result was confirmed by the pore size analysis and theoretical calculations, as presented in Appendix A Figs. S4,S5. The interior of NS is mainly composed of mesoporous particles with the diameter of 2 – 50 nm, which is larger than the diameter of ethylparaben (< 1.0 nm). The adsorbed ethylparaben could readily pass through the pores, thereby diffusing into the interior of NS minerals. (3) With the increase in the number of ethylparaben molecules entering the interior of NS, the free path of the ethylparaben molecules became narrower, which might have hindered the diffusion process. Additionally, the electrostatic repulsion among ethylparaben molecules could also impede the diffusion process, slowing down the adsorption process until the equilibrium was reached. This mechanism further confirmed the above-

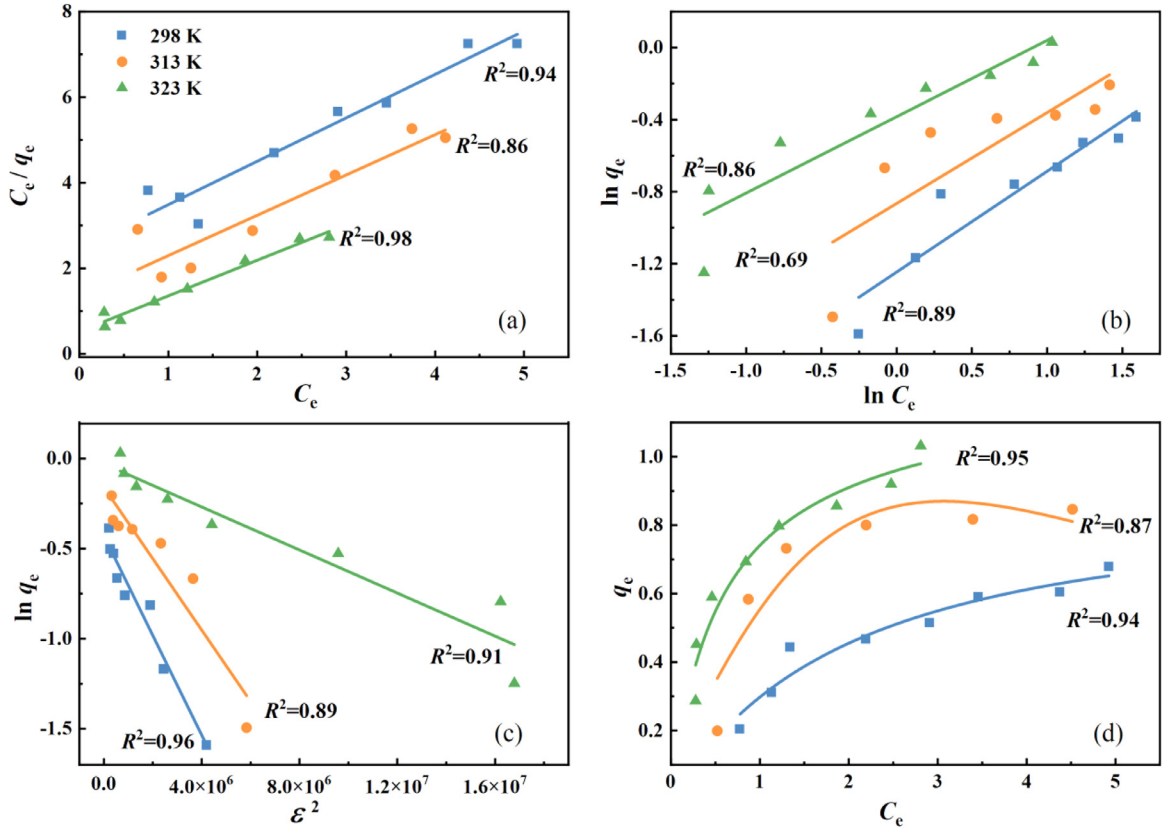

Fig. 3 – Langmuir (a); Freundlich (b); Dubinin-Radushkevich (c) and Redlich-Peterson (d) isotherm models for fitting of ethylparaben adsorption on NS at three different temperatures (298-313 K).

mentioned adsorption kinetics results. This means that the adsorption mainly occurred in the first stage, and the boundary layer diffusion was rapid on the external surface of NS. The rate constant was obtained and had the value of 0.14 [mg/ (g $hr^{0.5}$)], which was much larger than the latter two steps that had the rate constant values of k_{p2} = 0.035 and k_{p3} = 0.014 [mg/ (g $hr^{0.5}$)]. In short, both the surface adsorption and micropore filling could explain the adsorption of ethylparaben on NS minerals.

2.2. *Adsorption isotherms and thermodynamics*

In order to explore the binding patters between ethylparaben and the binding sites on NS, adsorption isotherm was fitted using different models, including Langmuir, Freundlich, Redlich–Peterson, and Dubinin–Radushkevich equations (Fig. 3). The four models are described in detail in Appendix A Text S3. The data presented in Table 2 shows the constants and correlation coefficients (R^2) obtained for the four isotherm models. The R^2 values of Freundlich isotherms were 0.89, 0.69, and 0.86 under the temperatures of 298, 313, and 323 K, respectively, which were lower than those for Langmuir (0.94, 0.86, and 0.98 for the temperatures of 298, 313, and 323 K, respectively) and Redlich–Peterson isotherms (0.94, 0.87, and 0.95 for the temperatures of 298, 313, and 323 K, respectively). These data suggest that Langmuir and Redlich–Peterson isotherms could fit better than the Freundlich isotherms. Nevertheless, the results for the Langmuir and Redlich–Peterson isotherms were almost indistinguishable. Due to this reason, a three-parameter adsorption isotherm, Redlich–Peterson correlation, was introduced. The Redlich–Peterson correlation combines the advantages of the two-parameter Langmuir and Freundlich isotherms. Generally, the exponent β in Redlich–Peterson isotherm has a value lying within the range of 0–1. There are two limiting behaviors, including Henry's law equation (β = 0) and Langmuir form (β = 1) (Redlich and Peterson, 1959). For the adsorption of ethylparaben on NS (Table 2), the Redlich–Peterson exponent β was calculated to have a value within the range of 0.93–0.95 within the temperature range of 298–323 K. The β value approaching unity suggests that Langmuir model was the most suitable one to describe the adsorption isotherms (Chen et al., 2020). Therefore, the results implied that the adsorption of ethylparaben on the surface of NS occurred through monolayer adsorption.

It is well known that Dubinin–Radushkevich isotherm is often employed to explore the adsorption mechanism with a free energy (E) and to distinguish the physical adsorption from chemical adsorption (Gunay et al., 2007). It is also accepted that the Dubinin–Radushkevich model can be successfully fit high activities of solutes (Ibrahim and Sani, 2014). In this study (Table 2), the Dubinin–Radushkevich model can also satisfactorily fit the experimental data (R^2 = 0.96, 0.89, and 0.91), which was consistent with the obtained kinetic results for the contribution of NS's micropores. Moreover, the calculated free energies of adsorption (E) values lied within the range of 0.95–

Table 2 – Parameters and correlation coefficients for four isotherm models of ethylparaben adsorption on NS.

Isotherms	Solution temperature (K)	Constants			R^2
		$q_{m(cal)}$ (mg/g)	$q_{m(exp)}$ (mg/g)	K_L (L/mg)	
Langmuir, $q_e = \frac{q_m k_1 C_e}{1+k_1 C_e}$	298	0.99	0.68	0.41	0.94
	313	1.06	0.81	1.06	0.86
	323	1.20	1.03	1.20	0.98
Isotherms	Solution temperature (K)	Constants			R^2
		K_f (mg^{1-n} L^n/g)	n		
Freundlich, $q_e = k_f C_e^{1/n}$	298	0.11	1.79		0.89
	313	0.18	1.98		0.69
	323	0.13	2.36		0.86
Isotherms	Solution temperature (K)	Constants			R^2
		a (mol^2/J^2)	E (kJ/mol)		
Dubinin-Radushkevich, $\ln q_e = \ln q_m - a\varepsilon^2$	298	2.77×10^{-7}	0.95		0.96
	313	2.08×10^{-7}	1.10		0.89
	323	5.98×10^{-8}	2.05		0.91
Isotherms	Solution temperature (K)	Constants			R^2
		k_{RP} (L/g)	α $(L/mg)^{\beta}$	β	
Redlich–Peterson, $q_e = \frac{k_{RP} C_e}{1+(\alpha C_e)^{\beta}}$	298	0.41	0.40	0.95	0.94
	313	1.90	2.53	0.93	0.87
	323	2.27	2.07	0.94	0.95

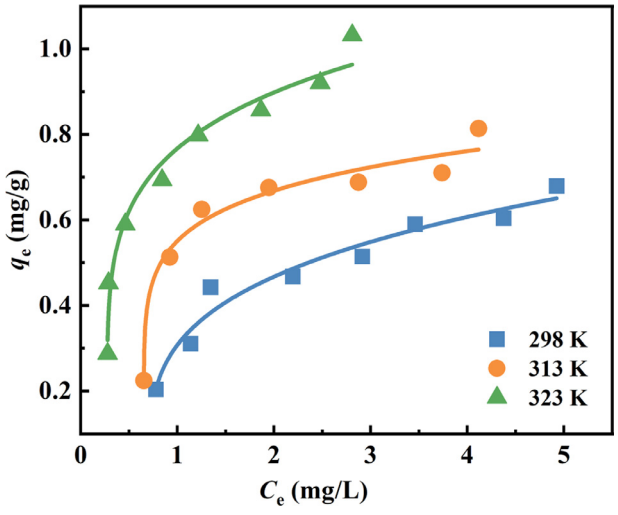

Fig. 4 – Ethylparaben adsorption isotherms on NS at three different temperatures (NS: 6 g/L, ethylparaben: 5 mg/L).

2.05 kJ/mol. Therefore, these data suggest that the adsorption of ethylparaben on NS could be mainly controlled by physical adsorption and non-covalent interactions.

Additionally, the rising temperature could enhance the adsorption of ethylparaben on NS. The maximum adsorption capacity (q_m) increased from 0.68 to 1.03 mg/g as the water temperature increased from 298 to 323 K, as shown in Fig. 4. Furthermore, a separation factor R_L in Langmuir isotherm can express the favorable adsorption (Hall et al., 1966). A lower R_L value reflects that the adsorption is more favorable. In this study, the calculated R_L values were 0.33, 0.16, and 0.14 for the temperatures of 298, 313, and 323 K, respectively. All the R_L values were less than unity, indicating favorable adsorption of ethylparaben on NS. Furthermore, the R_L value declined with the increase in temperature, indicating that the ongoing adsorption process was more favorable at higher temperatures. Moreover, the calculated thermodynamic parameters of ethylparaben adsorption on NS are presented in Appendix A Table S1. Due to positive ΔG (2.21 kJ/mol), the non-spontaneous adsorption occurred at the temperature of 298 K. However, with the increase in temperature, the ΔG values changed to −0.51 and −0.49 kJ/mol for the temperatures of 313 and 323 K, respectively, implying that the adsorption on NS could be spontaneous for temperatures higher than 313 K.

2.3. *Adsorption mechanism*

NS consists of mineral components and some organic matter, with ZnS nanoparticles as one of its major components (Li et al., 2020). Unexpectedly, no adsorption of ethylparaben was observed on pure ZnS nanoparticles (Appendix A Fig. S6), even though its surface area of 14.52 m^2/g is 10 times higher than that of NS minerals (1.22 m^2/g) (Appendix A Fig. S7 and Table S2). Therefore, ZnS particles were not mainly responsible for the adsorption of parabens on NS. However, the opposite case was observed in our previous research on the antibiotic-resistance genes (ARG) (Li et al., 2020), which

showed that ZnS nanoparticles could promote the transfer of ARG with the same efficiency as NS.

On the other hand, the content of organic matter of NS minerals was measured to lie within the range of 0.20–0.21% (Appendix A Table S3). According to a previous work (Schwarzenbach and Westall, 1981), the value above 0.1% suggests that the natural organic matter on NS could have contributed to the adsorption of hydrophobic ethylparaben. Therefore, hydrophobic partitioning into organic matter could largely govern the adsorption of ethylparaben on NS. Additionally, the critical role of organic matter on the surface of minerals is also experimentally demonstrated (Isaacson and Frink, 1984; Piatt et al., 1996). For instance, the migration and transformation processes of hydrophobic organic compounds from water to soil through adsorption have been experimental demonstrated (Chiou et al., 1979; Zhu and Chen, 2000). Due to this reason, in the current work, the adsorption of ethylparaben on NS was dominated by the partition of solutes to NS organic matter, which means that the hydrophobic organic pollutants can be distributed to the organic matter through dissolution, and the equilibrium can be achieved after a certain time period.

In order to evaluate the stability of ethylparaben adsorbed on NS, the desorption kinetics and adsorption capacity of ethylparaben on NS were further evaluated. The results show that no ethylparaben was detected in the desorption experiments, even with the extended desorption time of 5 days. This means that the desorption of ethylparaben from NS could be very difficult and was not released from NS once captured. Furthermore, to check the stability of NS, the irradiation of visible light was introduced due to the excellent visible-light photocatalytic activity of NS (Chen et al., 2011; Wang et al., 2017; Xia et al., 2013). The photochemical degradation of ethylparaben in the presence of NS was investigated under the irradiation of both the visible light and the simulated sunlight. Surprisingly, no significant change in ethylparaben concentration (< 2%) was observed upon irradiation of visible light (Appendix A Fig. S8). This data suggests that the ethylparaben adsorbed on NS was very stable to visible light and simulated sunlight. The adsorbed ethylparaben was difficult to be released to aquatic environments again and did not react with NS even upon irradiation, revealing the stability of adsorbed minerals. Based on our previous work (Chen et al., 2011), it can be inferred that the conduction band electrons (e^-), acting as the main reactive species (RSs), play an important role in the NS photocatalytic reaction upon irradiation of visible light. However, parabens have the very low activity for the electron transfer reaction, as demonstrated in our earlier experimental and theoretical researches (Fang et al., 2013; Gao et al., 2014; Gao et al., 2016). Therefore, it could explain that ethylparaben was actually adsorbed on NS rather than degraded under the irradiation of visible light and simulated sunlight.

3. Conclusions

This study shows that ethylparaben can be readily adsorbed on NS minerals. In particular, the adsorption process was a spontaneous process under the water temperature of more than 313 K. The sorption mainly occurred through surface adsorption along with micropore filling. Weber-Morris model satisfactorily explained the three-step adsorption process, whereas the main adsorption occurred in the initial stages of adsorption on the external surface of NS. The adsorption of ethylparaben on the surface of NS occurred through monolayer, physical and non-covalent interactions. Unexpectedly, the organic matter of NS (rather than the ZnS present in it) played a significant role in the adsorption of ethylparaben on NS. Furthermore, ethylparaben adsorbed onto NS minerals was stable, even though NS had excellent visible-light photocatalytic activity. The desorption and photochemical degradation were almost negligible, and had values of less than 2%. The findings of this research implied that the transformation and fate of EOCs can be significantly affected by natural minerals, and the remediation of EOCs-contaminated water using natural minerals should receive further research attention in the future.

Acknowledgments

The authors appreciate the financial supports from the National Natural Science Foundation of China (Nos. 41977365 and 41425015), the National Key Research and Development Program of China (No. 2019YFC1804503), the Local Innovative and Research Teams Project of Guangdong Pearl River Talents Program (No. 2017BT01Z032). Natural Sciences and Engineering Research Council of Canada, the Canada Research Chairs Program, Alberta Innovates, and Alberta Health for their support. YG acknowledges the support of Guangdong University of Technology for her visiting scholarship.

Appendix A Supplementary data

Supplementary material associated with this article can be found, in the online version, at doi:10.1016/j.jes.2021.05.030.

REFERENCES

Aharoni, C., Tompkins, F., 1970. Kinetics of Adsorption and Desorption and the Elovich Equation, Advances in Catalysis. Elsevier, pp. 1–49.

An, T., Fang, H., Li, G., Wang, S., Yao, S., 2014. Experimental and theoretical insights into photochemical transformation kinetics and mechanisms of aqueous propylparaben and risk assessment of its degradation products. Environ. Toxicol. Chem. 33, 1809–1816.

Bian, Y., Wang, D., Liu, X., Yang, Q., Liu, Y., Wang, Q., et al., 2020. The fate and impact of TCC in nitrifying cultures. Water Res. 178, 115851.

Brausch, J.M., Rand, G.M., 2011. A review of personal care products in the aquatic environment: environmental concentrations and toxicity. Chemosphere 82, 1518–1532.

Chen, L., Feng, W., Fan, J., Zhang, K., Gu, Z., 2020. Removal of silver nanoparticles in aqueous solution by activated sludge: mechanism and characteristics. Sci. Total Environ. 711, 135155.

Chen, Y., Deng, P., Xie, P., Shang, R., Wang, Z., Wang, S., 2017. Heat-activated persulfate oxidation of methyl- and ethyl-parabens: effect, kinetics, and mechanism. Chemosphere 168, 1628–1636.

Chen, Y., Lu, A., Li, Y., Zhang, L., Yip, H.Y., Zhao, H., et al., 2011. Naturally occurring sphalerite as a novel cost-effective photocatalyst for bacterial disinfection under visible light. Environ. Sci. Technol. 45, 5689–5695.
Cheng, W., Marsac, R., Hanna, K., 2018. Influence of magnetite stoichiometry on the binding of emerging organic contaminants. Environ. Sci. Technol. 52, 467–473.
Chiou, C.T., Peters, L.J., Freed, V.H., 1979. A physical concept of soil-water equilibria for nonionic organic compounds. Science 206, 831–832.
Darbre, P.D., Harvey, P.W., 2008. Paraben esters: review of recent studies of endocrine toxicity, absorption, esterase and human exposure, and discussion of potential human health risks. J. Appl. Toxicol. 28, 561–578.
Dobrin, D., Magureanu, M., Bradu, C., Mandache, N.B., Ionita, P., Parvulescu, V.I., 2014. Degradation of methylparaben in water by corona plasma coupled with ozonation. Environ. Sci. Pollut. Res. 21, 12190–12197.
Dubinin, M., 1947. The equation of the characteristic curve of activated charcoal. Proc. Acad. Sci. Phys. Chem. Sec. USSR55, 331-333, 875–890.
Eren, Z., Acar, F.N., 2006. Adsorption of Reactive Black 5 from an aqueous solution: equilibrium and kinetic studies. Desalination 194, 1–10.
Fang, H., Gao, Y., Li, G., An, J., Wong, P.K., Fu, H., et al., 2013. Advanced oxidation kinetics and mechanism of preservative propylparaben degradation in aqueous suspension of TiO_2 and risk assessment of its degradation products. Environ. Sci. Technol. 47, 2704–2712.
Freundlich, H., 1906. Über die adsorption in lösungen. Z. Phys. Chem. 57, 385–470.
Frisch, M.J., Trucks, G.W., Schlegel, H.B., Scuseria, G.E., Robb, M.A., Cheeseman, J.R., et al., 2009. Gaussian 09. Gaussian 09. Gaussian, Inc, Wallingford, CT, USA.
Frontistis, Z., Antonopoulou, M., Yazirdagi, M., Kilinc, Z., Konstantinou, I., Katsaounis, A., et al., 2017. Boron-doped diamond electrooxidation of ethyl paraben: the effect of electrolyte on by-products distribution and mechanisms. J. Environ. Manag. 195, 148–156.
Gao, Y., An, T., Fang, H., Ji, Y., Li, G., 2014. Computational consideration on advanced oxidation degradation of phenolic preservative, methylparaben, in water: mechanisms, kinetics, and toxicity assessments. J. Hazard. Mater. 278, 417–425.
Gao, Y., Ji, Y., Li, G., An, T., 2016. Theoretical investigation on the kinetics and mechanisms of hydroxyl radical-induced transformation of parabens and its consequences for toxicity: influence of alkyl-chain length. Water Res. 91, 77–85.
Gao, Y., Niu, X., Qin, Y., Guo, T., Ji, Y., Li, G., et al., 2020. Unexpected culprit of increased estrogenic effects: oligomers in the photodegradation of preservative ethylparaben in water. Water Res. 176, 115745.
Ghaffar, A., Ghosh, S., Li, F., Dong, X., Zhang, D., Wu, M., et al., 2015. Effect of biochar aging on surface characteristics and adsorption behavior of dialkyl phthalates. Environ. Pollut. 206, 502–509.
González-Mariño, I., Quintana, J.B., Rodríguez, I., Cela, R., 2011. Evaluation of the occurrence and biodegradation of parabens and halogenated by-products in wastewater by accurate-mass liquid chromatography-quadrupole-time-of-flight-mass spectrometry (LC-QTOF-MS). Water Res. 45, 6770–6780.
Gunay, A., Arslankaya, E., Tosun, I., 2007. Lead removal from aqueous solution by natural and pretreated clinoptilolite: adsorption equilibrium and kinetics. J. Hazard. Mater. 146, 362–371.
Hall, K.R., Eagleton, L.C., Acrivos, A., Vermeulen, T., 1966. Pore-and solid-diffusion kinetics in fixed-bed adsorption under constant-pattern conditions. Ind. Eng. Chem. Fundam. 5, 212–223.
Haman, C., Dauchy, X., Rosin, C., Munoz, J.F., 2015. Occurrence, fate and behavior of parabens in aquatic environments: a review. Water Res. 68, 1–11.
Ho, Y.S., 2003. Removal of copper ions from aqueous solution by tree fern. Water Res. 37, 2323–2330.
Ibrahim, M., Sani, S., 2014. Comparative isotherms studies on adsorptive removal of Congo red from wastewater by watermelon rinds and neem-tree leaves. Open J. Phys. Chem. 4, 139.
Isaacson, P.J., Frink, C.R., 1984. Nonreversible sorption of phenolic compounds by sediment fractions: the role of sediment organic matter. Environ. Sci. Technol. 18, 43–48.
Kasprzyk-Hordern, B., Dinsdale, R.M., Guwy, A.J., 2008. The occurrence of pharmaceuticals, personal care products, endocrine disruptors and illicit drugs in surface water in South Wales, UK. Water Res. 42, 3498–3518.
Li, G., Chen, X., Yin, H., Wang, W., Wong, P.K., An, T., 2020. Natural sphalerite nanoparticles can accelerate horizontal transfer of plasmid-mediated antibiotic-resistance genes. Environ. Int. 136, 105497.
Li, Y., Lu, A., Jin, S., Wang, C., 2009. Photo-reductive decolorization of an azo dye by natural sphalerite: case study of a new type of visible light-sensitized photocatalyst. J. Hazard. Mater. 170, 479–486.
Liao, C., Lee, S., Moon, H.B., Yamashita, N., Kannan, K., 2013. Parabens in sediment and sewage sludge from the United States, Japan, and Korea: spatial distribution and temporal trends. Environ. Sci. Technol. 47, 10895–10902.
Mitch, W.A., 2017. New takes on emerging contaminants: preface. J. Environ. Sci. 62, 1–2.
Oleszczuk, P., Pan, B., Xing, B., 2009. Adsorption and desorption of oxytetracycline and carbamazepine by multiwalled carbon nanotubes. Environ. Sci. Technol. 43, 9167–9173.
Petala, A., Frontistis, Z., Antonopoulou, M., Konstantinou, I., Kondarides, D.I., Mantzavinos, D., 2015. Kinetics of ethyl paraben degradation by simulated solar radiation in the presence of N-doped TiO_2 catalysts. Water Res. 81, 157–166.
Piatt, J.J., Backhus, D.A., Capel, P.D., Eisenreich, S.J., 1996. Temperature-dependent sorption of naphthalene, phenanthrene, and pyrene to low organic carbon aquifer sediments. Environ. Sci. Technol. 30, 751–760.
Prasad, M., Saxena, S., Amritphale, S.S., Chandra, N., 2000. Kinetics and isotherms for aqueous lead adsorption by natural minerals. Ind. Eng. Chem. Res. 39, 3034–3037.
Ramaswamy, B.R., Kim, J.W., Isobe, T., Chang, K.H., Amano, A., Miller, T.W., et al., 2011. Determination of preservative and antimicrobial compounds in fish from Manila Bay, Philippines using ultra high performance liquid chromatography tandem mass spectrometry, and assessment of human dietary exposure. J. Hazard. Mater. 192, 1739–1745.
Redlich, O., Peterson, D.L., 1959. A useful adsorption isotherm. J. Phys. Chem. 63, 1024.
Rytwo, G., Mendelovits, A., Eliyahu, D., Pitcovski, J., Aizenshtein, E., 2010. Adsoption of two vaccine-related proteins to montmorillonite and organo-montmorillonite. Appl. Clay Sci. 50, 569–575.
Kumar, S.N., 2015. The Study of Oil Spillage Clean Up using Polymers. PhD thesis.
Schwarzenbach, R.P., Egli, T., Hofstetter, T.B., von Gunten, U., Wehrli, B., 2010. Global water pollution and human health. Annu. Rev. Env. Resour. 35, 109–136.
Schwarzenbach, R.P., Westall, J., 1981. Transport of nonpolar organic compounds from surface water to groundwater. Laboratory sorption studies. Environ. Sci. Technol. 15, 1360–1367.
Shen, C., Gu, X., Yang, B., Zhang, D., Wang, Z., Shu, Z., et al., 2020. Mineralogical characteristics and photocatalytic properties of natural sphalerite from China. J. Environ. Sci. 89, 156–166.

Sustic, A., 1995. Functional polymers 60. Chemical structure/ultraviolet spectrum relationship of 2(2-hydroxyphenyl)2H-benzotriazoles: synthesis of novel 2(2-hydroxyphenyl)2H-benzotriazoles. Polymer 36 (17), 3401–3408 (Guildf).

Tan, I.A., Ahmad, A.L., Hameed, B.H., 2009. Adsorption isotherms, kinetics, thermodynamics and desorption studies of 2,4,6-trichlorophenol on oil palm empty fruit bunch-based activated carbon. J. Hazard. Mater. 164, 473–482.

Tanis, E., Hanna, K., Emmanuel, E., 2008. Experimental and modeling studies of sorption of tetracycline onto iron oxides-coated quartz. Colloids Surf. A Physicochem. Eng. Asp. 327, 57–63.

Wang, B., Wu, D., Chu, K.H., Ye, L., Yip, H.Y., Cai, Z., et al., 2017. Removal of harmful alga, Chattonella marina, by recyclable natural magnetic sphalerite. J. Hazard. Mater. 324, 498–506.

Xia, D., Ng, T.W., An, T., Li, G., Li, Y., Yip, H.Y., et al., 2013. A recyclable mineral catalyst for visible-light-driven photocatalytic inactivation of bacteria: natural magnetic sphalerite. Environ. Sci. Technol. 47, 11166–11173.

Yan, L., Anhuai, L., Changqiu, W., 2006. Photocatalytic reduction of CrVI by natural sphalerite suspensions under visible light irradiation. Acta Geol. Sin. 80, 267–272.

Yang, X.G., Li, Y., Lu, A.H., Yan, Y.H., Wang, C.Q., Wong, P.K., 2011. Photocatalytic reduction of carbon tetrachloride by natural sphalerite under visible light irradiation. Sol. Energy Mat. Sol. Cells 95, 1915–1921.

Zhao, Y., Liu, F., Wang, M., Qin, X., 2020. Oxidation of diclofenac by birnessite: identification of products and proposed transformation pathway. J. Environ. Sci. 98, 169–178.

Zhu, L., Chen, B., 2000. Sorption behavior ofp-Nitrophenol on the Interface between anion−cation organobentonite and water. Environ. Sci. Technol. 34, 2997–3002.